RSC Advances

ROYAL SOCIETY OF CHEMISTRY

www.rsc.org/advances

RSC Advances

RSCPublishing

PAPER

Light emission property and self-assembly of a tolane-based luminogen†

Cite this: DOI: 10.1039/xoxxoooooox

Ying Zang, Yi Li, Baozong Li, Hongkun Li* and Yonggang Yang*

Received ooth January 2012,
Accepted ooth January 2012

DOI: 10.1039/xoxxoooooox

www.rsc.org/

The self-assembly of π-conjugated molecules into low-dimensional luminescent nanomaterials has attracted much attention for their applications in optoelectronic and photonics. Herein, a new tolane derivative (**1**) containing donor and acceptor units has been designed and synthesized. The compound **1** shows the effect of intramolecular charge transfer (ICT) due to the donor-acceptor interaction. In solution, it is weakly emissive, but becomes highly emissive upon aggregation, demonstrating the novel phenomenon of aggregation-induced emission (AIE). Moreover, through controlled self-assembly of **1**, different micro/nanostructures (ribbons, rods and flower-like clusters) with high emission efficiency can be obtained, which paves the way for its photonic and electronic applications.

Introduction

Because of their unique optical properties and potential applications in optoelectronics and biological fields, the construction of organic luminescent materials with micro/nano structures through self-assembly of π-conjugated molecules has drawn increasing interest in recent years.[1] Unfortunately, most of the traditional organic luminophores suffer from the effect of aggregation-caused quenching (ACQ).[2] They emit strong fluorescence in their dilute solution, but become weakly emissive or even non-emissive in the condensed state due to the formation of the detrimental excimers or exciplexes. Since the luminescent materials are inevitably made into thin films or bulk solids, the ACQ effect thus greatly limits their practical applications. To circumvent the ACQ problem, a new type of luminescent molecules with aggregation-induced emission (AIE) characteristics have recently been developed.[3] AIE fluorogens, such as tetraphenylethylene (TPE),[4] silole,[5] distyrylanthracene,[6] triphenylethene[7], and their derivatives, exhibit weak or no emission in their dilute solutions, but become highly luminescent in the aggregate state. Restriction of intramolecular motions (RIM) processes are proposed as the main cause for the AIE phenomena.[8] The novel photophysical properties make AIE luminogens promising candidates for constructing efficient fluorescent micro/nanomaterials.

There have been research efforts to fabricate luminescent supramolecular architectures through self-assembly of AIE molecules.[9] For instance, Zheng prepared fluorescent nanofibers and nanospheres by the aggregation of TPE-containing macrocyclic compounds.[10] Liang and Zhou fabricated the luminescent micelles through self-assembly of TPE-modified polyethylene glycol.[11] Ouyang and coworkers have reported the controlled self-assembly of electron-donor-substituted AIE compounds into different emission colors and morphologies (microblocks, microparticles, microrods, and nanowires).[12] Šket constructed the luminescent microfibers by the sublimation process of a BF_2 complex.[13] Huang synthesized two four-armed TPE derivatives containing electron-rich and electron-deficient groups, which can form the luminescent one-dimensional (1D) nanorods by the charge-transfer interactions.[14] Sun and Tang obtained well-defined 1D micro/nano-structures (fibers, wires, rods and ribbons) with bright fluorescence through the self-assembly of TPE-functionalized perylene bisimides and fumaronitriles.[15] Recently, Li and Tang prepared amino acid-containing TPEs, which are capable of self-assembling into helical micro/nanofibers with enhanced emission.[16] However, the reported self-assembly systems with AIE property are mainly based on TPE derivatives. It is thus highly desired to develop new AIE fluorogens and investigate their self-assembly behaviors.

Although tolane derivatives have been widely studied in liquid crystals,[17] their photoluminescence properties have been less explored.[18] In this work, we report the light emission property and self-assembly behavior of a tolane derivative (**1**) bearing donor (D) and acceptor (A) units. The tolane-based luminogen shows the characteristics of intramolecular charge transfer (ICT) and AIE. The molecule can self-assemble into different ordered micro/nanostructures such as ribbons, rods and flowers under controlled solvent, temperature and concentration. The obtained microstructures emit bright blue fluorescence and exhibit obvious optical waveguide effect.

Experimental section

General information

1,3-Dicyclohexylcarbodiimde (DCC) was purchased from Suzhou Highfine Biotech Co., Ltd. (China). Dichloromethane (DCM), Tetrahydrofuran (THF), *N*,*N*-Dimethylformamide (DMF), toluene, acetonitrile and ethanol were obtained from

Sinopharm Group Chemical Reagent Co., Ltd. (China) and purified by standard methods immediately prior to use.

FTIR spectra were taken on a Nicolet 6700 spectrometer at 2 cm^{-1} resolution by averaging over 32 scans. The ^1H NMR spectrum was recorded on a Varian NMR (400 MHz) spectrometer in DMSO-d_6 solutions using tetramethylsilane (TMS) as an internal standard. Elemental analysis was performed on a Perkin Elmer series II CHNS/O analyzer 2400. UV-vis absorption spectra were recorded on a Shimadzu UV-3150. The photoluminescence (PL) spectra were taken on an Edinburgh FLS-920 with a Xe-900 lamp as excitation source. The particle size distribution was measured on a Malvern Zetasizer Nano ZS. Field emission scanning electron microscopy (FE-SEM) images were taken on a Hitachi S-4800 operating at 3.0 kV. Wide angle X-ray diffraction (WAXRD) patterns were recorded on an X′ Pert-Pro MPD X-ray diffractometer using Cu Kα radiation with a Ni filter (1.542 Å). The fluorescence micrograph image was taken on an inverted fluorescence microscope (Nikon Eclipse TE2000-U).

Sample preparation for PL measurement

A stock acetonitrile solution of **1** with a concentration of 100 μM was first prepared. Aliquots of the stock solution were transferred to 10 mL volumetric flasks. After appropriate amounts of acetonitrile were added, distilled water was added dropwisely under vigorous stirring to afford 10 μM solutions with different water fractions (0–90 vol%). The PL measurements of the resulting solutions were then conducted immediately.

Synthesis

4-[(4-methoxyphenyl)ethynyl]benzoic acid (**2**) was synthesized according to the literature.[19]

Synthesis of N-cyclohexyl-N-(cyclohexylcarbamoyl)-4-[(4-methoxyphenyl)ethynyl]benzamide (**1**). Compound **2** (1.00 g, 3.96 mmol) and DCC (0.98 g, 4.75 mmol) were dissolved in THF (200 mL) under stirring. The reaction mixture was kept at 0 ℃ for 3 h under N_2 and room temperature for another 24h. The resulting reaction mixture was filtered. The filtrate was evaporated to get crude product. Compound **1** was purified on a silica gel column using dichloromethane-methanol mixture (50:1, v/v) as eluent and recrystallized from ethanol. Yield: 19.3 %, (350 mg). FT-IR (KBr): 3470 cm^{-1} (ν_{N-H}, free), 3288 and 3070 cm^{-1} (ν_{N-H}, associate), 3057 cm^{-1}(C-H of the phenyl, stretching), 2932 cm^{-1} (ν_{asC-H}) , 2854 cm^{-1} (ν_{sC-H}), 2214 cm^{-1} ($\nu_{C\equiv C}$), 1667 cm^{-1} ($\nu_{C=O}$), 1600 cm^{-1}, 1512 cm^{-1}, 1452 cm^{-1} (ν_{Ar}), 1540 cm^{-1} (δ_{C-N-H}). ^1H-NMR (400 MHz, DMSO-d_6, 25 ºC), δ (TMS, ppm): 1.13-1.88 (m, 20H; -C$\underline{H_2}$-), 3.25-3.27 (m, 1H; C$\underline{H}$NH), 4.24-4.30 (m, 1H; C$\underline{H}$N), 3.89 (s, 3H; OC$\underline{H_3}$), 7.07-7.10 (d, 2H, J = 8.8 Hz; 2,6-Ph$\underline{H}$OCH$_3$), 7.57-7.63 (m, 6H; 3,5-Ph$\underline{H}$OCH$_3$, 2,3,5,6-Ph$\underline{H}$C≡C), 8.03-8.04 (d, 1H, J = 5.2 Hz; CHN$\underline{H}$). Elemental analysis calcd (%): C, 75.95; H, 7.47; N, 6.11; found: C, 75.56; H, 7.72; N, 5.83.

Results and discussion

The molecular structure of **1** and its synthesis route are shown in Scheme 1. It was easily synthesized by a one-step reaction. The product was carefully purified and characterized by spectroscopic methods and elemental analysis, from which satisfactory results corresponding to its molecular structures were obtained. The detailed synthesis procedure and structure characterization data are given in the Experimental Section.

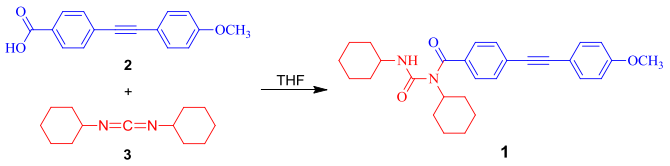

Scheme 1 Synthetic route to the compound **1**.

Optical properties

The molecule **1** is composed of electron-donating methoxy group and electron-accepting carbonyl group. As we know, the fluorophores with electron D-A structures could form ICT process, which is often associated with a red-shift in the emission color and a decrease in the emission intensity with increasing solvent polarity.[20] We thus investigated the absorption and emission properties of **1** in the solvents with different polarities.

As shown in Fig. 1a, **1** exhibits a similar absorption profile with a peak at ~310 nm in the different solvents, suggesting that the solvent polarity has not much influence on its absorbance property. The normalized emission spectral profiles of **1** in the solvents (Fig. 1b) are, however, different due to the solvent polarity-dependent ICT attribute. In weakly polar toluene and moderately polar THF, **1** gives the emission peaks at 375 and 393 nm, respectively, whose emissions occur from the locally excited state. In highly polar solvents like DMF, ethanol and acetonitrile, the emission peaks are red-shifted to about 454 nm, demonstrating the ICT state emission is predominant. Evidently, **1** shows ICT feature.

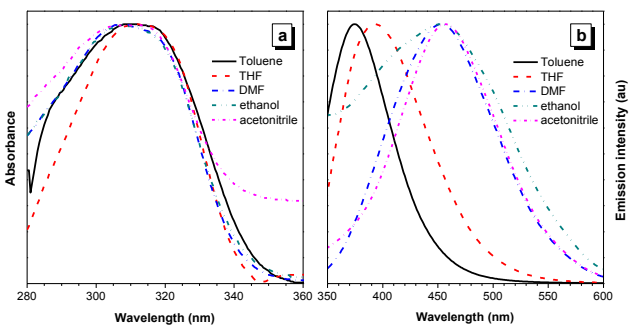

Fig. 1 Normalized (a) absorption and (b) emission spectra of **1** in different solvents. Concentration: 10 μm. Solutions were excited at their absorption maxima.

A tolane derivative with an alkoxy group was recently reported to be AIE active.[18a] To check whether **1** still remains the AIE characteristic with introduction of an D-A structure, we studied its emission behaviors in the solution and aggregation state. Since the compound **1** is easily soluble in acetonitrile but insoluble in water, we then measured the PL spectra of **1** in the acetonitrile/water mixtures with different water fractions (f_w). As depicted in Fig. 2a, **1** shows blue fluorescence with a peak at 456 nm in pure acetonitrile. The emission intensity is progressively decreased with gradual addition of water into its acetonitrile solution (f_w < 70%). Meanwhile, the emission maximum red-shifts to 475 nm. This is a typical ICT process caused by the increased solvent polarity. When f_w is above 70%, the emissions blue-shift to 394 nm and intensify significantly. The highest intensity was recorded at the f_w of 90%, which is 3-fold higher than that in pure acetonitrile solution (Fig. 2b). That is to say, **1** is also AIE-active.

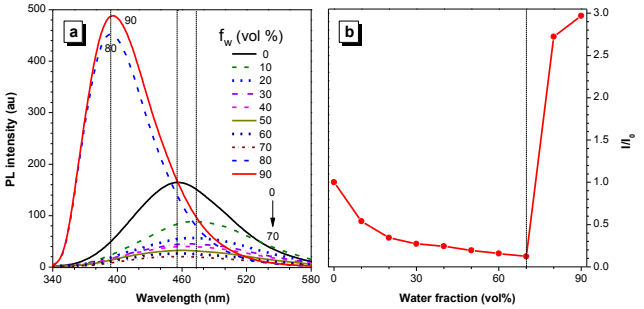

Fig. 2 PL spectra of **1** in acetonitrile/water mixtures with different water fractions (f_w). Concentration: 10 μM; excitation wavelength: 305 nm. (B) Plot of relative emission peak intensity (I/I_0) versus f_w of the acetonitrile-water mixtures, where I = emission intensity and I_0 = emission intensity in acetonitrile solution.

As we know, water is more polar than acetonitrile. The polarity of the acetonitrile/water mixtures increases with increasing water content. When f_w is below 70%, the sufficient aggregates of **1** are not formed. This is proved by the particle size results, which show no signal in the mixture with low f_w values (Fig. S1, ESI†). With addition of water to the acetonitrile solution of **1** (f_w < 70%), the emissions of the mixtures become gradually weak and red-shift induced by the increased polarity, suggesting the ICT effect dominates the light emission behavior. Since water is poor solvent for **1**, the molecules must be aggregated at high water fractions in the mixture. This is the case. At f_w > 70%, the aggregates are generated, which is supported by the particle size data: particles with diameters more than 200 nm are found in the mixtures (Fig. S1, ESI†). It is further proved by the level-off tails observed in the longer wavelength region in the UV spectra of the mixtures with high f_w values (Fig. S2, ESI†). Such phenomena are generally seen in the nanoparticle suspensions due to the light scattering effect of the aggregates. The RIM effect thus overwhelms the ICT effect in the aggregated state, which blocks the nonradiative relaxation channels and turns on the emission of the molecules.[8] Meanwhile, the emissions are blue-shifted in the aggregated state. This may be due to the less polar environment inside the aggregates[20b] or the decrease in the solvent effect on the emission behaviors of the aggregates.[21] Therefore, **1** exhibits both ICT and AIE characteristics in the acetonitrile-water mixtures with different water fractions.

Self-assembly behaviors

Molecular self-assembly is an efficient bottom-up approach in fabricating ordered micro/nano-structure materials. The driving forces are mainly the intermolecular interactions, such as hydrogen bonding, electrostatic interactions, π-π stacking, and solvophobic interactions. Recently, the D-A dipole-dipole interaction between ICT molecules have been used to assemble nanostructures.[1c, 22] Considering that **1** possesses both ICT and AIE characteristics, it is anticipated to form well-defined nanostructures with high emission in proper conditions. The self-assembly behaviors of **1** in different conditions were thus studied using FE-SEM.

We first examined the morphologies of **1** upon the evaporation of its ethanol solution with the concentrations ranging from 2.5 mg mL^{-1} to 10 mg mL^{-1} at room temperature. As displayed in Fig. 3, SEM images show the formation of microribbons with the length of several micrometers and width from 0.1 to 1 μm. Interestingly, the microribbons further assemble into flower-like clusters at high concentrations (Fig. 3c, d).

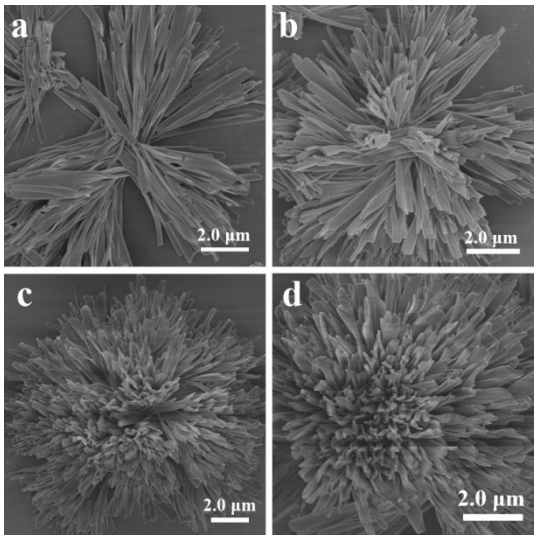

Fig. 3 SEM images of **1** generated by evaporation of its ethanol solution with concentrations of (a) 2.5 mg mL^{-1}, (b) 5 mg mL^{-1}, (c) 7.5 mg mL^{-1} and (d) 10 mg mL^{-1} at room temperature.

The temperature generally greatly influences the morphologies of nanostructures. We then investigated the self-assembly behaviors of **1** in ethanol with different concentrations at 0 °C. After being dried in air on glass flakes at concentrations from 5 to 10 mg mL^{-1} in ethanol, radial crystals were obtained (Fig. 4). Taking the microstructures formed in 10 mg mL^{-1} of ethanol as an example, these radially rectangular pyramids which are about 5.0-8.0 μm in length and 1.0-3.0 μm in diameter. The WAXRD pattern shows many sharp peaks at 2θ of 7-40 °, indicating a crystalline structure (Fig. S3, ESI†).

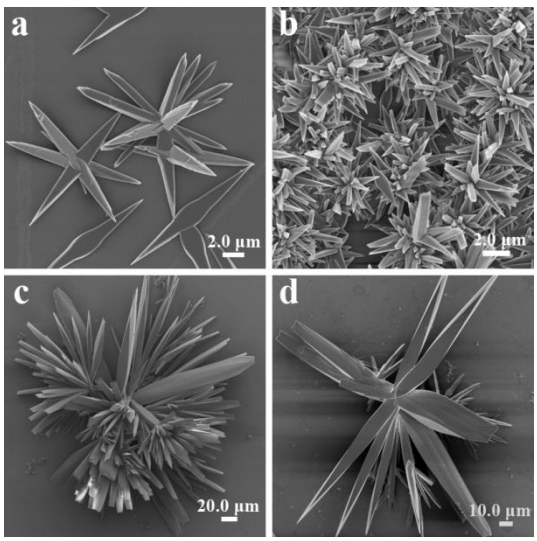

Fig. 4 SEM images of **1** formed by evaporation of its ethanol solution with concentrations of (a and b) 10 mg mL^{-1}, (c) 7.5 mg mL^{-1} and (d) 5 mg mL^{-1} 0 °C .

When the concentration was decreased to 2.5 mg mL^{-1}, bundles of twisted nanoribbons were identified (Fig. 5a, b). These nanoribbons are about 500-900 nm in width, 90-110 nm in thickness, 6.0-15.0 μm in length. Their helical pitches were

about 5.0-7.0 μm. Its WAXRD pattern (Fig. S3, ESI†) exhibits only several peaks at 2θ of 7-40°, indicating a partially crystalline structure. Interestingly, helical ribbons were observed (Fig. 5c), whose width, thickness and length are about 400-700 nm, 30-60 nm and 4.0-9.0 μm, respectively. The helical pitches are about 0.5-1.0 μm. The helical structures prompt us to investigate the optical active properties of the aggregates. However, no obvious circular dichroism (CD) signals were observed in the CD spectra of the aggregates of **1** generated by evaporation of its ethanol solution with a concentration of 2.5 mg mL^{-1} at 0 ℃ (Fig. S5, ESI†). This indicates that equal numbers of left and right-handed ribbons are formed. It is known that both the increase of entropy and the decrease of surface free energy could drive nanomaterials to form helical morphologies.[23] Since molecule **1** has a bent-core structure and banana-shaped molecules tend to organize into helical structures, the helical self-assembly of **1** might be directed by this conformational chirality.[24] Furthermore, the formed microcrystals emit blue light upon UV excitation (Fig. 5d). Glaring light emissions were observed at the ends of the microcrystals (highlighted by the red circles), exhibiting their optical waveguide effect. We also studied its self-assembly behaviors in other solvents with a concentration of 10 mg mL^{-1} at 0 ℃. Radial crystals were also generated in isopropanol (Fig. S4a, ESI†). In *n*-propanol and THF, it can self-assemble into nanoribbons and nanorods (Fig. S4b, c and d, ESI†), respectively. The results demonstrate that the molecule **1** possesses strong self-assembly ability. The self-assembly and optical waveguiding properties of **1** thus make it a promising candidate for application in optoelectronic nanodevices.[25]

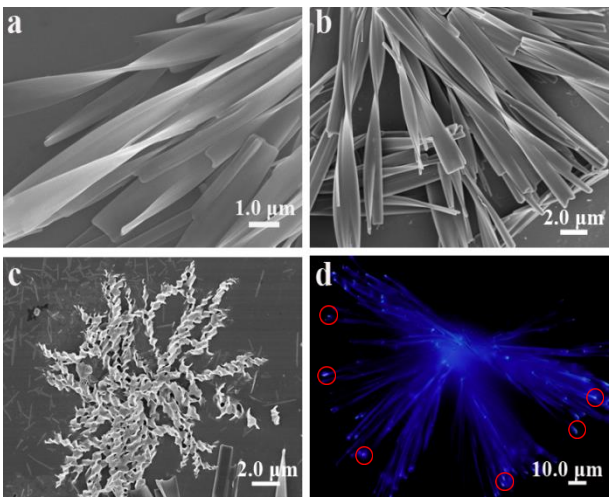

Fig. 5 SEM (a, b and c) and fluorescent (d) images of **1** formed by evaporation of its ethanol solution with a concentration of 2.5 mg mL^{-1} at 0 °C.

Since **1** contains amide group, there may be hydrogen bonding interactions between the molecules, which control the micro/nanostructures growth together with D-A dipole-dipole interaction.[22b] To check it, the FT-IR spectra of **1** in the twisted micro/nanostructures prepared at concentrations of 2.5 and 10 mg mL^{-1} in ethanol were recorded (Fig. 6). For the twisted nanoribbons formed at a concentration of 2.5 mg mL^{-1}, the broad band at around 3470 cm^{-1} is associated with the stretching vibrations of N-H of the "free" amide groups, while the absorption band at around 3288 cm^{-1} is stemmed from the stretching vibrations of N-H of the hydrogen-bonded amide groups. Furthermore, the stretching vibration band of C=O was observed at around 1667 cm^{-1}, which shifts to lower wavenumbers. The results indicate that the intermolecular hydrogen-bonding interaction affects the stacking of the molecules. The FT-IR spectrum of the radial crystals formed at 10 mg mL^{-1} was similar to that of the twisted ribbons generated at 2.5 mg mL^{-1}, suggesting that the driving forces for the micro/nanostructures are the same. Therefore, the self-assembly processes of **1** are controlled by the cooperative interactions of D-A and hydrogen bonding.

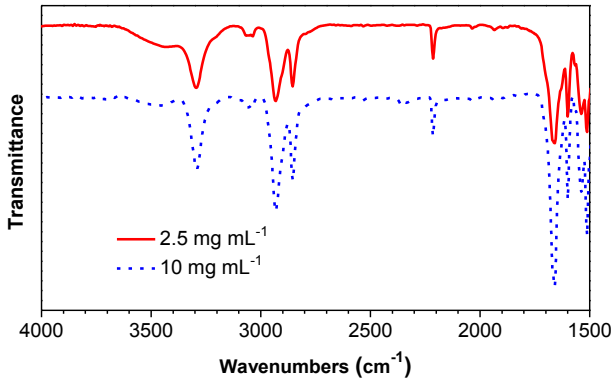

Fig. 6 FT-IR spectra of **1** formed by evaporation of its ethanol solution with concentrations of 2.5 and 10 mg mL^{-1} at 0 °C.

Conclusions

In summary, we have successfully synthesized a new tolane-based fluorogen containing a D-A structure (**1**) by a one-step reaction. The fluorogen shows the solvent polarity-dependent ICT effect and AIE characteristic. Through controlling the experimental conditions, such as temperature, solvents and concentrations, various ordered micro/nanostructures are generated by the assembling of **1** upon the synergistic D-A and hydrogen-bonding interactions. The fluorogen can form microribbons and flower-like clusters in ethanol at room temperature. In THF, it grows into nanorods at 0 ℃. **1** can self-assemble into radical crystals at the concentrations of 5~10 mg mL^{-1}, while it forms twisted and helical micro/nanoribbons at a concentration of 2.5 mg mL^{-1} in ethanol at 0 ℃. Moreover, the obtained microstructures exhibit bright blue fluorescence and obvious optical waveguide effect. Such properties make it an attractive material for optoelectronic and photonics applications.

Acknowledgements

This work was supported by the Natural Science Foundation of Jiangsu Province (No. BK2011354), the Priority Academic Program Development of Jiangsu High Education Institutions (PAPD), and the National Natural Science Foundation of China (No. 51473106 and 21404077).

Notes and references

Jiangsu Key Laboratory of Advanced Functional Polymer Design and Application, College of Chemistry, Chemical Engineering and Materials Science, Soochow University, Suzhou 215123, China. E-mail: hkli@suda.edu.cn; ygyang@suda.edu.cn; Fax: +86-512-65882052; Tel: +86-512-65880047

†Electronic Supplementary Information (ESI) available: Particle size (Fig. S1) and UV spectra (Fig. S2) of **1** in acetonitrile/water mixtures, WAXRD patterns of **1** formed by evaporation of its ethanol solution (Fig.

S3), SEM images of **1** formed by evaporation of its isopropanol, n-propanol and THF solutions (Fig. S4), CD spectrum of **1** in aggregate state (Fig. S5). See DOI: 10.1039/b000000x/

1 (a) A. Kaeser and A. P. H. J. Schenning, *Adv. Mater*., 2010, **22**, 2985; (b) L. Magginia and D. Bonifazi, *Chem. Soc. Rev*., 2012, **41**, 211; (c) Y. Li, T. Liu, H. Liu, M. Z. Tian and Y. Li, *Acc. Chem. Res.*, 2014, **47**, 1186.

2. J. B. Birks, *Photophysics of Aromatic Molecules*, Wiley, New York, 1970.

3 (a) Y. Hong, J. W. Y. Lam and B. Z. Tang, *Chem. Commun.*, 2009, 4332; (b) Y. Hong, J. W. Y. Lam and B. Z. Tang, *Chem. Soc. Rev.*, 2011, **40**, 5361; (c) D. Ding, K. Li, B. Liu and B. Z. Tang, *Acc. Chem. Res.*, 2013, **46**, 2441.

4 (a) Z. Zhao, J. W. Y. Lam and B. Z. Tang, *J. Mater. Chem.*, 2012, **22**, 23726; (b) J. Huang, N. Sun, Y. Dong, R. Tang, P. Lu, P. Cai, Q. Li, D. Ma, J. Qin and Z. Li, *Adv. Funct. Mater*., 2013, **23**, 2329; (c) W.-L. Gong, B. Wang, M. P. Aldred, C. Li, G.-F. Zhang, T. Chen, L. Wang and M.-Q. Zhu, *J. Mater. Chem. C*, 2014, **2**, 7001; (d) D. G. Khandare, H. Joshi, M. Banerjee, M. S. Majikb and A. Chatterjee, *RSC Adv.*, 2014, **4**, 47076; (e) Y. Lin, G. Chen, L. Zhao, W. Z. Yuan, Y. Zhang and B. Z. Tang, *J. Mater. Chem. C*, 2015, **3**, 112; (f) T. Jiang, Y. Qu, B. Li, Y. Gao and J. Hua, *RSC Adv.*, 2015, **5**, 1500.

5 (a) J. Liu, J. W. Y. Lam and B. Z. Tang, *J. Inorg. Organomet. Polym. Mater*., 2009, **19**, 249; (b) J. Mei, J. Wang, J. Z. Sun, H. Zhao, W. Z. Yuan, C. M. Deng, S. M. Chen, H. H. Y. Sung, P. Lu, A. J. Qin, H. S. kwok, Y. G. Ma, I. D. Williams and B. Z. Tang, *Chem. Sci*., 2012, **3**, 549; (c) L. Chen, Y. Jiang, H. Nie, P. Lu, H. H. Y. Sung, I. D. Williams, H. S. Kwok, F. Huang, A. Qin, Z. Zhao and B. Z. Tang, *Adv. Funct. Mater*., 2014, **24**, 3621.

6 (a) B. Xu, J. B. Zhang, S. Ma, J. Chen, Y. Dong and W. Tian, *Prog. Chem*., 2013, **25**, 1079; (b) J. B. Zhang, B. Xu, J. L. Chen, S. Q. Ma, Y. J. Dong, L. J. Wang, B. Li, L. Ye and W. J. Tian, *Adv. Mater.*, 2014, **26**, 739; (c) S. Xue, W. Liu, X. Qiu, Y. Gao and W. Yang, *J. Phys. Chem. C*, 2014, **118**, 18668.

7 (a) Z. Yang, Z. Chi, T. Yu, X. Zhang, M. Chen, B. Xu, S. Liu, Y. Zhang and J. Xu, *J. Mater. Chem.*, 2009, **19**, 5541; (b) Z. Chi, X. Zhang, B. Xu, X. Zhou, C. Ma, Y. Zhang, S. Liu, J. Xu, *Chem. Soc. Rev.*, 2012, **41**, 3878.

8 (a) E. P. J. Parrott, N. Y. Tan, R. Hu, J. A. Zeitler, B. Z. Tang and E. Pickwell-MacPherson, *Mater. Horiz.*, 2014, **1**, 251; (b) J. Mei, Y. Hong, J. W. Y. Lam, A. Qin, Y. Tang and B. Z. Tang, *Adv. Mater.*, 2014, **26**, 5429.

9 (a) B. K. An, J. Gierschner and S. Y. Park, *Acc. Chem. Res.*, 2012, **45**, 544; (b) Z. Zhao, J. W. Y. Lam and B. Z. Tang, *Soft Matter*, 2013, **9**, 4564; (c) C. Shi, Z. Guo, Y. Yan, S. Zhu, Y. Xie, Y. S. Zhao, W. Zhu and H. Tian, *ACS Appl. Mater. Interfaces*, 2013, **5**, 192; (d) R. Hu, J. W. Y. Lam, H. Deng, Z. Song, C. Zheng and B. Z. Tang, *J. Mater. Chem. C*, 2014, **2**, 6326; (e) E. Wang, J. W. Y. Lam, R. Hu, C. Zhang, Y. S. Zhao and B. Z. Tang, *J. Mater. Chem. C*, 2014, **2**, 1801; (f) D. Belei, C. Dumea, E. Bicua and L. Marin, *RSC Adv.*, 2015, **5**, 8849.

10 H. T. Feng, S. Song, Y. C. Chen, C. H. Shen and Y. S. Zheng, *J. Mater. Chem. C*, 2014, **2**, 2353.

11 C. Zhang, S. Jin, S. Li, X. Xue, J. Liu, Y. Huang, Y. Jiang, W.-Q. Chen, G. Zou and X.-J. Liang, *ACS Appl. Mater. Interfaces*, 2014, **6**, 5212.

12 C. Niu, L. Zhao, T. Fang, X. Deng, H. Ma, J. Zhang, N. Na, J. Han and J. Ouyang, *Langmuir*, 2014, **30**, 2351.

13 P. Galer, R. C. Korošec, M. Vidmar and B. Šket, *J. Am. Chem. Soc.*, 2014, **136**, 7383.

14 G. Yu, G. Tang and F. Huang, *J. Mater. Chem. C*, 2014, **2**, 6609.

15 (a) Q. Zhao, S. Zhang, Y. Liu, J. Mei, S. Chen, P. Lu, A. Qin, Y. Ma, J. Z. Sun and B. Z. Tang, *J. Mater. Chem.*, 2012, **22**, 7387; (b) X. Y. Shen, W. Z. Yuan, Y. Liu, Q. Zhao, P. Lu, Y. Ma, I. D. Williams, A. Qin, J. Z. Sun and B. Z. Tang, *J. Phys. Chem. C*, 2013, **117**, 7334.

16 (a) H. Li, J. Cheng, Y. Zhao, J. W. Y. Lam, K. S. Wong, H. Wu, B. S. Li and B. Z. Tang, *Mater. Horiz.*, 2014, **1**, 518; (b) H. Li, J. Cheng, H. Deng, E. Zhao, B. Shen, J. W. Y. Lam, K. S. Wong, H. Wu, B. S. Li and B. Z. Tang, *J. Mater. Chem. C*, 2015, **3**, 2399.

17 (a) A. S. Matharu, S. Jeeva and P. S. Ramanujam, *Chem. Soc. Rev.*, 2007, **36**, 1868; (b) D. Zhao, W. Huang, H. Cao, Y. Zheng, G. Wang, Z. Yang and H. Yang, *J. Phys. Chem. B*, 2009, **113**, 2961; (c) W. Z. Yuan, Z.-Q. Yu, P. Lu, C. Deng, J. W. Y. Lam, Z. Wang, E.-Q. Chen, Y. Ma and B. Z. Tang, *J. Mater. Chem.*, 2012, **22**, 3323.

18 (a) Y. Chen, J. Lin, W. Z. Yuan, Z. Yu, J. W. Y. Lam and B. Z. Tang, *Sci. China Chem.*, 2013, **56**, 1191; (b) S.-J. Wang, R.-Y. Zhao, S. Yang, Z.-Q. Yu and E.-Q. Chen, *Chem. Commun.*, 2014, **50**, 8378.

19 C. J. Wenthur, R. Morrison, A. S. Felts, K. A. Smith, J. L. Engers, F. W. Byers, J. S. Daniels, K. A. Emmitte, P. J. Conn and C. W. Lindsley, *J. Med. Chem.*, 2013, **56**, 5208.

20 (a) Z. R. Grabowski and K. Rotkiewicz, *Chem. Rev.*, 2003, **103**, 3899; (b) R. Hu, E. Lager, A. Aguilar-Aguilar, J. Liu, J. W. Y. Lam, H. H. Y. Sung, I. D. Williams, Y. Zhong, K. S. Wong, E. Pena-Cabrera and B. Z. Tang, *J. Phys. Chem. C*, 2009, **113**, 15845; (c) W. Z. Yuan, Y. Gong, S. Chen, X. Y. Shen, J. W. Y. Lam, P. Lu, Y. Lu, Z. Wang, R. Hu, N. Xie, H. S. Kwok, Y. Zhang, J. Z. Sun and B. Z. Tang, *Chem. Mater.*, 2012, **24**, 1518.

21 Z. Yang, W. Qin, J. W. Y. Lam, S. Chen, H. H. Y. Sung, I. D. Williams and B. Z. Tang, *Chem. Sci.*, 2013, **4**, 3725.

22 (a) X. Zhang, X. Zhang, W. Shi, X. Meng, C. Lee and S. Lee, *Angew. Chem., Int. Ed.*, 2007, **46**, 1525; (b) B. J. Jordan, Y. Ofir, D. Patra, S. T. Caldwell, A. Kennedy, S. Joubanian, G. Rabani, G. Cooke and V. M. Rotello, *Small*, 2008, **4**, 2074; (c) J. Xu, X. Liu, J. Lv, M. Zhu, C. Huang, W. Zhou, X. Yin, H. Liu, Y. Li and J. Ye, *Langmuir*, 2008, **24**, 4231; (d) S. Chen, Z. Qin, T. Liu, X. Wu, Y. Li, H. Liu, Y. Song and Y. Li, *Phys. Chem. Chem. Phys.*, 2013, **15**, 12660.

23 (a) Y. Snir and R. D. Kamien, *Science*, 2005, **307**, 1067; (b) S. Yang, L. Zhao, C. Yu, X. Zhou, J. Tang, P. Yuan, D. Chen and D. Zhao, *J. Am. Chem. Soc.*, 2006, **128**, 10460.

24 M. Cano, A. Sánchez-Ferrer, J. L. Serrano, N. Gimeno and M. B. Ros, *Angew. Chem. Int. Ed.*, 2014, **53**, 13449.

25 Y. Yan and Y. S. Zhao, *Chem. Soc. Rev.*, 2014, **43**, 4325.